Rayleigh waves on a superlattice stratified normal to the surface

B. Djafari-Rouhani
Laboratoire des Surfaces et Interfaces, Institut Superieur d'Electronique du Nord, Lille Cedex, France

A. A. Maradudin and R. F. Wallis
Department of Physics, University of California, Irvine, California 92717

(Received 8 February 1984)

We present a theory of Rayleigh waves on a superlattice when the surface is perpendicular to the alternating layers. The method consists of first Fourier analyzing the equations of motion in the direction perpendicular to the layers so as to include automatically the boundary conditions at the different interfaces. For each value of the wave vector k perpendicular to the layers, this gives a set of wave vectors parallel to the layers, i.e., perpendicular to the surface. Then a surface wave is constructed from a superposition of these solutions. The frequencies of the surface Rayleigh waves are obtained by using the Fourier-analyzed conditions of vanishing stresses at the free surface. Numerical calculations are performed by limiting the number of Fourier components taken into account. For two relatively similar layers in the superlattice there are two different Rayleigh branches near the Brillouin-zone boundary which result from the folding of the dispersion curve for a Rayleigh wave on a homogeneous medium. The higher branch can disappear when the two layers differ significantly in their elastic properties. We present a few examples of the dispersion curves and of the associated displacement fields. We also present examples showing the variation of the gap between the two Rayleigh branches versus the parameters of the layers and their thicknesses.

I. INTRODUCTION

Despite a great deal of work on the propagation of acoustic waves in layered media[1,2] there is still considerable interest in this problem at the present time due to the possibility of fabricating superlattices that consist of alternating layers of two different materials.[3,4] Although the bulk properties of such superlattices are being studied intensely at the present time,[5] a great deal of attention has been directed recently at the magnetic,[5-7] electromagnetic,[5,8] and vibrational[5,9-16] properties of *semi-infinite* superlattices. In this last case, the possibility of Love-type waves has been demonstrated,[9] and explicit expressions for their dispersion have been derived.[13,14] The dispersion of Rayleigh waves on such superlattices has also been obtained in explicit form.[15] Finally, the surface modes of a superlattice have been studied on the basis of atomic models.[12]

In this paper we present what is to our knowledge the first study of the propagation of Rayleigh waves on a superlattice cut normal to its laminations (Fig. 1). In the direction x_1 perpendicular to the layers the Brillouin zone for this structure is limited to $-\pi/a < k < \pi/a$, where k is the wave vector of the Rayleigh wave and a is the period of the superlattice. The restricted range of variation of k gives rise to a bending of the Rayleigh-wave dispersion curve near the zone boundary (wave slowing), as well as to the possibility of a second, higher-frequency branch of the dispersion curve in a limited frequency range, due to the folding of the dispersion curve for Rayleigh waves on a homogeneous medium back into the first Brillouin zone. Similar effects occur for a medium homogeneous in the bulk, but containing periodic surface perturbations in the direction of propagation of the Rayleigh wave, such as a grating.[17]

In Sec. II we shall describe the theory which gives the frequencies of the Rayleigh waves on this type of superlattice. In this method the equations of motion are Fourier-analyzed in the x_1 direction in order to automatically include the boundary conditions at the different interfaces between the layers. The Rayleigh-wave frequencies are obtained by seeking a surface wave satisfying the Fourier-analyzed boundary conditions at the free surface.

Section III is devoted to some applications of this theory. A few dispersion curves, as well as the associated displacement fields are presented, and the effects of the physical parameters of the layers and their thicknesses on the two branches of the Rayleigh-wave dispersion curve near the zone boundary are discussed. Some conclusions from this study are presented in Sec. IV.

II. THEORY OF RAYLEIGH WAVES ON VERTICALLY STRATIFIED MEDIA

A. General presentation

The geometry of the superlattice studied in this paper is depicted in Fig. 1. The two layers are assumed to be elastic, isotropic or cubic, media characterized by the elastic moduli c_{11},c_{12},c_{44} and c'_{11},c'_{12},c'_{44} and their densities ρ and ρ', respectively. In the case of cubic media the theory presented below applies when the free surface is a (001) surface, and the x_1-axis surface is along [100]. In the case of isotropic media the additional assumption is made that each medium has only two independent elastic constants as a consequence of the relations $c_{11}=c_{12}+2c_{44}$

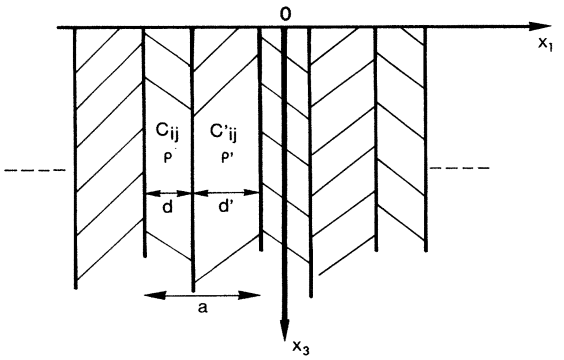

FIG. 1. Geometry of the semi-infinite superlattice.

and $c'_{11}=c'_{12}+2c'_{44}$.

As indicated in Fig. 1, the free surface is perpendicular to the x_3 direction, and we assume that the wave vector k parallel to the surface is in the x_1 direction. The period of the superlattice is $a=d+d'$, where d and d' are the thicknesses of the unprimed and primed media, respectively. In this paper we are interested in surface waves polarized in the sagittal plane (the x_1,x_3 plane). As a matter of fact, these waves are decoupled (for the symmetry considered in this paper) from the so-called transverse, or shear horizontal, modes polarized along x_2.

The method that we will use to obtain these waves is based on a Fourier analysis, along x_1, of the equations of motion in the bulk, which includes the boundary conditions at the different interfaces separating the layers; this is achieved by taking the elastic moduli c_{ij} and the density ρ to be coordinate dependent. For given values of ω and k this operation leads to an infinite set of equations which has an infinite number of solutions for the wave vector k_3 along x_3. If at least one of these solutions is real, this means that one can find at that frequency a wave propagating in the superlattice. On the other hand, if all k_3 are imaginary or complex, this frequency is situated outside the bulk bands. Then one can construct a surface wave by taking a combination of those solutions which have a decaying behavior far from the surface. Finally, this surface wave should satisfy the conditions for vanishing stresses at the free surface, which are also Fourier-analyzed and which give rise to a set of linear homogeneous equations. The Rayleigh-wave frequencies are then obtained by equating the determinant associated with this system to zero.

The numerical analyses are of course done by limiting the number of equations in the above-mentioned sets; this means that we take a finite number of Fourier components. We now turn to details of the theory.

B. Theoretical description

The equation of motion of an elastic medium can be written in the form

$$\rho\frac{\partial^2 u_\alpha(\vec{x},t)}{\partial t^2}=\sum_\beta\frac{\partial T_{\alpha\beta}(\vec{x},t)}{\partial x_\beta},\quad \alpha=1,2,3 \tag{2.1}$$

where $\vec{u}(\vec{x},t)$ is the displacement field, and the elements of the stress tensor $\overleftrightarrow{T}$ are given by

$$T_{\alpha\beta}=\sum_{\mu\nu}C_{\alpha\beta\mu\nu}(\vec{x})\frac{\partial u_\mu}{\partial x_\nu}(\vec{x},t)\ . \tag{2.2}$$

However, the elastic constants and the density are x_1 dependent, i.e., for example, $\rho(x_1)=\rho$ (ρ') if x_1 belongs to the medium 1 (2). Then, in the contracted Voigt notation, the equations of motion for cubic materials with (001) surfaces and k along [100] become

$$\begin{aligned}-\omega^2\rho(x_1)u_1=&\frac{\partial c_{11}(x_1)}{\partial x_1}\frac{\partial u_1}{\partial x_1}+\frac{\partial c_{12}(x_1)}{\partial x_1}\frac{\partial u_3}{\partial x_3}\\&+c_{11}(x_1)\frac{\partial^2 u_1}{\partial x_1^2}+c_{44}(x_1)\frac{\partial^2 u_1}{\partial x_3^2}\\&+[c_{12}(x_1)+c_{44}(x_1)]\frac{\partial^2 u_3}{\partial x_1\partial x_3}\ ,\end{aligned} \tag{2.3a}$$

$$\begin{aligned}-\omega^2\rho(x_1)u_3=&\frac{\partial c_{44}(x_1)}{\partial x_1}\left[\frac{\partial u_1}{\partial x_3}+\frac{\partial u_3}{\partial x_1}\right]\\&+[c_{44}(x_1)+c_{12}(x_1)]\frac{\partial^2 u_1}{\partial x_1\partial x_3}\\&+c_{44}(x_1)\frac{\partial^2 u_3}{\partial x_1^2}+c_{11}(x_1)\frac{\partial^2 u_3}{\partial x_3^2}\ .\end{aligned} \tag{2.3b}$$

In Eqs. (2.3) we have assumed a harmonic time dependence of the displacement field

$$u_\alpha(\vec{x},t)=u_\alpha(\vec{x})e^{-i\omega t}\ . \tag{2.4}$$

We now expand all periodic functions of x_1 in a Fourier series. For example, the density can be written

$$\rho(x_1)=\sum_{j=-\infty}^{\infty}\hat{\rho}(j)e^{i(2\pi jx_1/a)}\ , \tag{2.5}$$

with

$$\hat{\rho}(j)=\frac{1}{a}\int_0^a dx_1\rho(x_1)e^{-i(2\pi jx_1/a)}\ . \tag{2.6}$$

The displacement components, however, must possess the Bloch property

$$u_\alpha(x_1,x_3)=\sum_{j=-\infty}^{\infty}\hat{u}_\alpha(j\,|\,x_3)e^{ik_jx_1}\ , \tag{2.7}$$

where

$$k_j=k+2\pi j/a\ . \tag{2.8}$$

We substitute these expressions into the equations of motion (2.3) and then equate the mth Fourier coefficients,

$$\sum_{n=-\infty}^{\infty}\left[\omega^2\hat{\rho}(m-n)-\frac{2\pi(m-n)}{a}\hat{c}_{11}(m-n)k_n-\hat{c}_{11}(m-n)k_n^2+\hat{c}_{44}(m-n)\frac{d^2}{dx_3^2}\right]\hat{u}_1(n\mid x_3)$$
$$+\sum_{n=-\infty}^{\infty} i\left[\frac{2\pi(m-n)}{a}\hat{c}_{12}(m-n)+[\hat{c}_{12}(m-n)+\hat{c}_{44}(m-n)]k_n\right]\frac{d}{dx_3}\hat{u}_3(n\mid x_3)=0,\quad m=0,\pm1,\pm2,\ldots \tag{2.9a}$$

$$\sum_{n=-\infty}^{\infty} i\left[\frac{2\pi(m-n)}{a}\hat{c}_{44}(m-n)+[\hat{c}_{12}(m-n)+\hat{c}_{44}(m-n)]k_n\right]\frac{d}{dx_3}\hat{u}_1(n\mid x_3)$$
$$+\sum_{n=-\infty}^{\infty}\left[\omega^2\hat{\rho}(m-n)-\frac{2\pi(m-n)}{a}\hat{c}_{44}(m-n)k_n-\hat{c}_{44}(m-n)k_n^2+\hat{c}_{11}(m-n)\frac{d^2}{dx_3^2}\right]\hat{u}_3(n\mid x_3)=0,\quad m=0,\pm1,\pm2,\ldots. \tag{2.9b}$$

It is worthwhile to note that these equations describe the motion of the elastic waves in each medium, but also fulfill the conditions of continuity at the interfaces.

To solve Eqs. (2.9) we assume

$$\hat{u}_1(n\mid x_3)=A_n e^{-\lambda x_3},\quad \hat{u}_3(n\mid x_3)=B_n e^{-\lambda x_3}, \tag{2.10}$$

with $\mathrm{Re}\lambda>0$ to ensure satisfaction of the boundary conditions at $x_3=\infty$. (The parameter λ is equivalent to ik_3, where k_3 is the wave vector along x_3.) Inserting the solutions (2.10) into Eqs. (2.9), we obtain the two following coupled sets of equations:

$$\sum_n\left[\omega^2\hat{\rho}(m-n)-\frac{2\pi(m-n)}{a}\hat{c}_{11}(m-n)k_n-\hat{c}_{11}(m-n)k_n^2+\hat{c}_{44}(m-n)\lambda^2\right]A_n$$
$$+\sum_n(-i\lambda)\left[\frac{2\pi(m-n)}{a}\hat{c}_{12}(m-n)+[\hat{c}_{12}(m-n)+\hat{c}_{44}(m-n)]k_n\right]B_n=0, \tag{2.11a}$$

$$\sum_n(-i\lambda)\left[\frac{2\pi(m-n)}{a}\hat{c}_{44}(m-n)+[\hat{c}_{12}(m-n)+\hat{c}_{44}(m-n)]k_n\right]A_n$$
$$+\sum_n\left[\omega^2\hat{\rho}(m-n)-\frac{2\pi(m-n)}{a}\hat{c}_{44}(m-n)k_n-\hat{c}_{44}(m-n)k_n^2+\hat{c}_{11}(m-n)\lambda^2\right]B_n=0,\quad m=0,\pm1,\pm2,\ldots. \tag{2.11b}$$

Let us introduce two column vectors $\vec{A}$ and $\vec{B}$ whose components are the coefficients A_n and B_n, respectively. Then one can formally write Eqs. (2.11) in the matrix form

$$(\overleftrightarrow{M}'_{11}\lambda^2+\overleftrightarrow{M}''_{11})\vec{A}-i\lambda\overleftrightarrow{M}_{13}\vec{B}=0, \tag{2.12a}$$

$$(-i\lambda)\overleftrightarrow{M}_{31}\vec{A}+(\overleftrightarrow{M}'_{33}\lambda^2+\overleftrightarrow{M}''_{33})\vec{B}=0, \tag{2.12b}$$

where the matrices $\overleftrightarrow{M}_{ij}$, $\overleftrightarrow{M}'_{ij}$, and $\overleftrightarrow{M}''_{ij}$ are independent of λ.

In order to solve this set of equations, we perform a simple transformation on it that reduces it to a standard eigenvalue problem. This consists of setting

$$\vec{\tilde{A}}=-\frac{1}{i\lambda}\vec{A},\quad \vec{\tilde{B}}=\vec{B}. \tag{2.13}$$

Then if we introduce the matrices

$$\overleftrightarrow{M}'=\begin{bmatrix}\overleftrightarrow{M}'_{11} & 0\\ -\overleftrightarrow{M}_{31} & \overleftrightarrow{M}'_{33}\end{bmatrix},\quad \overleftrightarrow{M}''=-\begin{bmatrix}\overleftrightarrow{M}''_{11} & \overleftrightarrow{M}_{13}\\ 0 & \overleftrightarrow{M}''_{33}\end{bmatrix}, \tag{2.14}$$

Eqs. (2.12) become

$$\lambda^2\overleftrightarrow{M}'\begin{bmatrix}\vec{\tilde{A}}\\ \vec{B}\end{bmatrix}=\overleftrightarrow{M}''\begin{bmatrix}\vec{\tilde{A}}\\ \vec{B}\end{bmatrix}. \tag{2.15}$$

Equation (2.15) indicates that the λ^2 are the eigenvalues of the matrix $\overleftrightarrow{M}'^{-1}\overleftrightarrow{M}''$ and that $(\vec{\tilde{A}},\vec{B})$ are the corresponding eigenvectors.

Finally, let us construct a surface wave by taking a linear combination of the above solutions, which we label by the index s:

$$\hat{u}_1(n\mid x_3)=\sum_s K_s A_{ns}(\lambda_s)e^{-\lambda_s x_3}, \tag{2.16a}$$

$$\hat{u}_3(n\mid x_3)=\sum_s K_s B_{ns}(\lambda_s)e^{-\lambda_s x_3}. \tag{2.16b}$$

This solution has to satisfy the conditions of vanishing stresses at the free surface $x_3=0$, which can be written

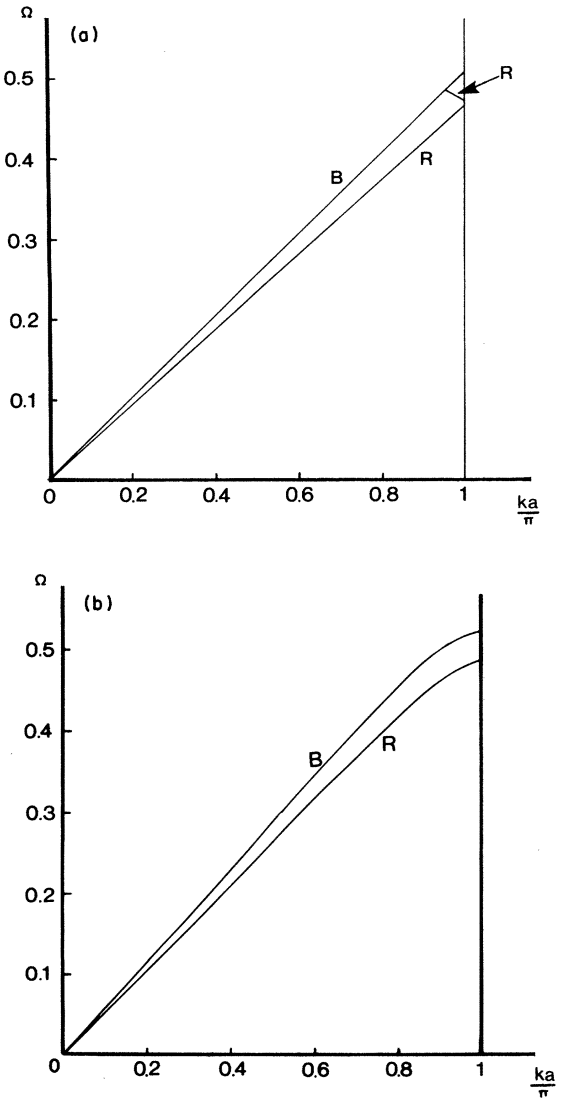

FIG. 2. Dispersion of the bottom of the bulk bands (B) and of the Rayleigh waves (R) in the reduced Brillouin zone associated with the superlattice. The two media in the superlattice differ only by their mass densities, with (a) $\rho'/\rho=0.95$ and (b) $\rho'/\rho=0.5$. Ω is a reduced frequency $\Omega=(\omega/c_t^0)(a/2\pi)$, where $c_t^0=(c_{44}/\rho)^{1/2}$ is the transverse speed of sound in the first medium.

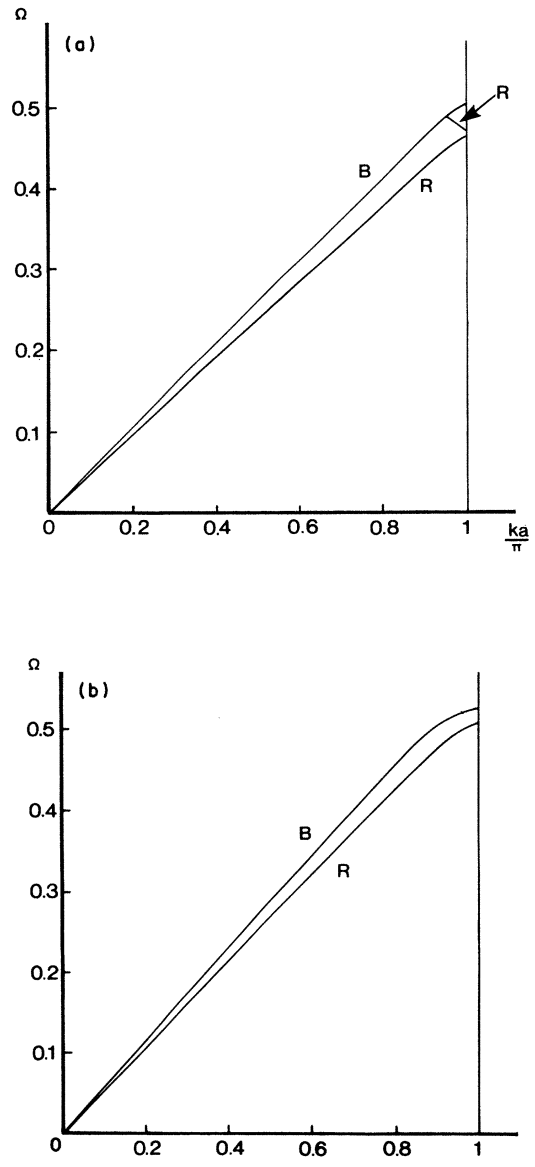

FIG. 3. Same as in Fig. 2 when the two media in the superlattice have the same mass densities, but elastic constants in the ratio (a) $c'_{44}/c_{44}=1.1$ or (b) 2.

TABLE I. Test for the convergence of the results when one increases the number of the Fourier coefficients involved in the calculations. The frequencies of the Rayleigh wave (index R) and of the bottom of the bulk bands (index B) are given in the reduced notation $\Omega=\omega a/2\pi c_t^0$, where $c_t^0=(c_{44}/\rho)^{1/2}$ is the transverse speed of sound for the first medium. The results are given when the two media in the superlattice differ only in their mass densities, with $\rho'/\rho=0.95$, or only in their elastic constants, with $c'_{44}/c_{44}=1.1$.

	Mass-density variation		Elastic-constant variation	
M	Ω_R	Ω_B	Ω_R	Ω_B
0	0.530 81	0.577 35	0.563 01	0.612 37
1	0.486 80	0.523 90	0.516 19	0.534 48
2	0.486 36	0.523 41	0.509 98	0.527 46
4	0.486 34	0.523 37	0.508 20	0.525 58
8	0.486 33	0.523 36	0.507 20	0.524 52
12	0.486 33	0.523 36	0.506 84	0.524 14

$$\left[c_{44}(x_1)\left[\frac{\partial u_1}{\partial x_3}+\frac{\partial u_3}{\partial x_1}\right]\right]_{x_3=0}=0\,, \tag{2.17a}$$

$$\left[c_{12}(x_1)\frac{\partial u_1}{\partial x_1}+c_{11}(x_1)\frac{\partial u_3}{\partial x_3}\right]_{x_3=0}=0\,. \tag{2.17b}$$

The Fourier expansion of Eqs. (2.17) yields the pair of equations

$$\left[\sum_{n=-\infty}^{\infty}\hat{c}_{44}(m-n)\times\left[\frac{d\hat{u}_1(n\mid x_3)}{dx_3}+ik_n\hat{u}_3(n\mid x_3)\right]\right]_{x_3=0}=0\,, \tag{2.18a}$$

$$\left[\sum_{n=-\infty}^{\infty}\left[\hat{c}_{12}(m-n)ik_n\hat{u}_1(n\mid x_3)+\hat{c}_{11}(m-n)\frac{d\hat{u}_3(n\mid x_3)}{dx_3}\right]\right]_{x_3=0}=0\,, \tag{2.18b}$$

with $m=0,\pm1,\pm2,\ldots$.

Inserting the solutions (2.16) into Eqs. (2.18) results in a pair of equations for the determination of the coefficients $\{K_s\}$:

$$\sum_s K_s\left[\sum_n\left[-\hat{c}_{44}(m-n)A_{ns}(\lambda_s)\lambda_s+i\hat{c}_{44}(m-n)k_nB_{ns}(\lambda_s)\right]\right]=0\,, \tag{2.19b}$$

$$\sum_s K_s\left[\sum_n\left[i\hat{c}_{12}(m-n)k_nA_{ns}(\lambda_s)-\hat{c}_{11}(m-n)B_{ns}(\lambda_s)\lambda_s\right]\right]=0\,, \tag{2.19b}$$

with $m=0,\pm1,\pm2,\ldots$.

The dispersion relation for the Rayleigh wave is obtained by equating the determinant of this linear system to zero. To obtain numerical results, it is necessary to limit the number of equations involved, i.e., to use a finite number of Fourier components. This will be done in the next section where the displacements are described by $2M+1$ terms in the Fourier expansions (2.7), that is, the summation on j in Eq. (2.7) [or the index n in Eq. (2.10)] range from $-M$ to $+M$. Then Eqs. (2.9), (2.11), (2.18), and (2.19) will be considered for $m=0,\pm1,\pm2,\ldots,\pm M$. We note that the matrices $\overleftrightarrow{M}'$ and $\overleftrightarrow{M}''$ [Eqs. (2.14)] are of order $2(2M+1)$, and thus this is also the number of values assumed by the index s in Eqs. (2.16) and (2.19).

III. DISPERSION CURVES AND DISPLACEMENTS FOR THE RAYLEIGH WAVES

This section is devoted to a few applications of the general theory presented in Sec. II. Unless otherwise specified, we assume that (i) the two elastic media are isotropic with the following relations among the elastic constants: $c_{44}=c_{12}=\frac{1}{3}c_{11}$; and (ii) the two layers have the same thickness: $d=d'$. Let us note that the velocity of the Rayleigh wave on a homogeneous medium with $c_{12}=c_{44}=\frac{1}{3}c_{11}$ is given by

$$c_R^2=2(1-\sqrt{3}/3)c_{44}/\rho\cong0.846c_{44}/\rho\,.$$

Most of the results presented in the following sections are obtained by taking M, which determines the number of the Fourier components involved in the calculation, to be $M=4$. This choice will be discussed later. However, in some figures we made the choice $M=8$ or even $M=12$ when, due to the large difference between the parameters of the two layers, the results deviate from the $M=4$ case by a detectable difference on the scale of the figures (of the order of 1%).

A. Dispersion curves for the Rayleigh waves

We first present the dispersion curves for the Rayleigh waves and the bottom of the bulk bands in the following cases. (i) The elastic moduli are independent of x_1 and the mass densities have the following ratios: (a) $\rho'/\rho=0.95$ [Fig. 2(a)]; (b) $\rho'/\rho=0.5$ [Fig. 2(b)]; (ii) the mass density is independent of x_1 and the elastic moduli have the following ratios: (a) $c'_{44}/c_{44}=1.1$ [Fig. 3(a)]; (b) $c'_{44}/c_{44}=2$ [Fig. 3(b)]. These curves are drawn for the case $M=4$. This choice comes from a test, summarized in Table I, on the convergence of the results when one increases the number of Fourier coefficients involved in the calculation. The test is done by varying M in cases (i b) and (ii b) above, when the wave vector k is at the Brillouin-zone boundary ($k=\pi/a$) where one could expect the slowest convergence. The convergence is faster when only the mass density is x_1 dependent. Let us also note that even small values of M give a good qualitative idea of the physical results, especially when the c_{ij} are x_1

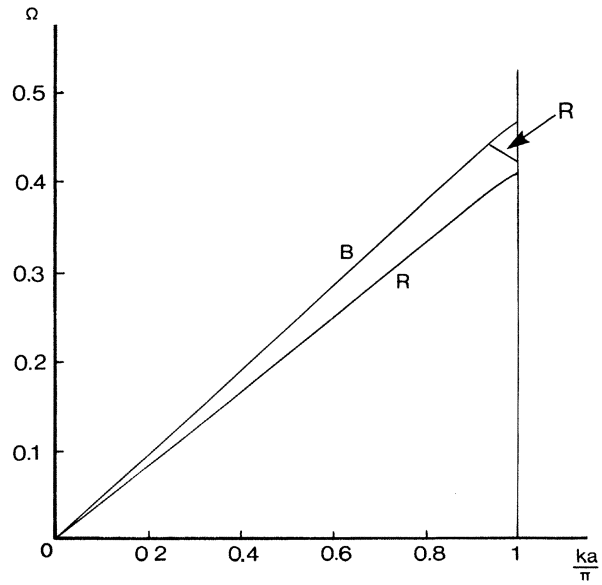

FIG. 4. Same as in Fig. 2 for a GaAs-$Ga_xAl_{1-x}As$—type superlattice. The elastic constants are assumed identical for the two media and $\rho'/\rho=0.9$. Here $c_t^0=c_t$ (GaAs).

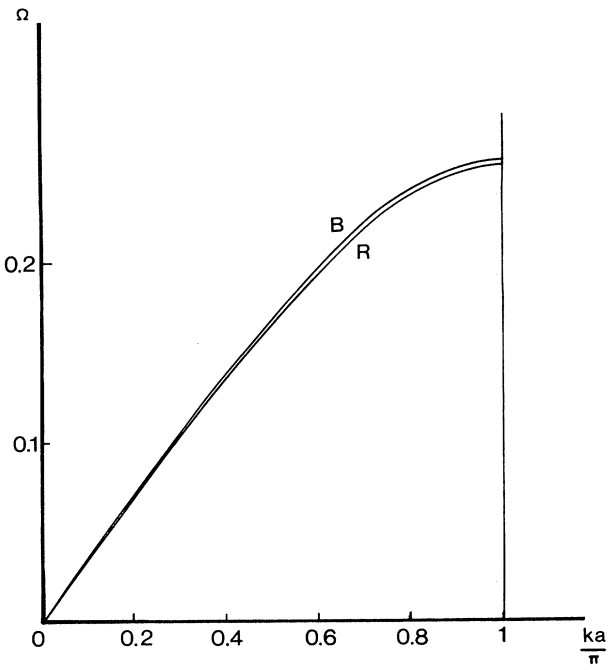

FIG. 5. Same as in Fig. 2 for a W-Al—type superlattice. Here $c_t^0 = c_t(\mathrm{W})$.

TABLE II. Elastic constants and densities of Al and W. The elastic constant $c_{12} = c_{11} - 2c_{44}$ satisfies the isotropy assumption.

	c_{11} (10^{10} N/m^2)	c_{44} (10^{10} N/m^2)	ρ (g/cm^3)
W	52.33	16.07	19.317
Al	10.68	2.82	2.733

independent; this comes from the fact that the lowest eigenvalues λ_s are not very much affected by the introduction of the higher Fourier components in the calculation.

Let us now make a few comments about Figs. 2 and 3. Near the Brillouin-zone boundary, there is a bending of the Rayleigh-wave dispersion curve (wave slowing), as well as of the bottom of the bulk bands; the difference between the two media is greater as the bending becomes larger. On the other hand, if one starts from a homogeneous medium and then introduces the superlattice by slightly changing medium 2 with respect to medium 1 [Figs. 2(a) and 3(a)], one observes a folding of the Rayleigh wave associated with the homogeneous medium; thus two surface wave branches are present near the zone boundary. When the difference between the densities (or the elastic constants) of the two media increases, the

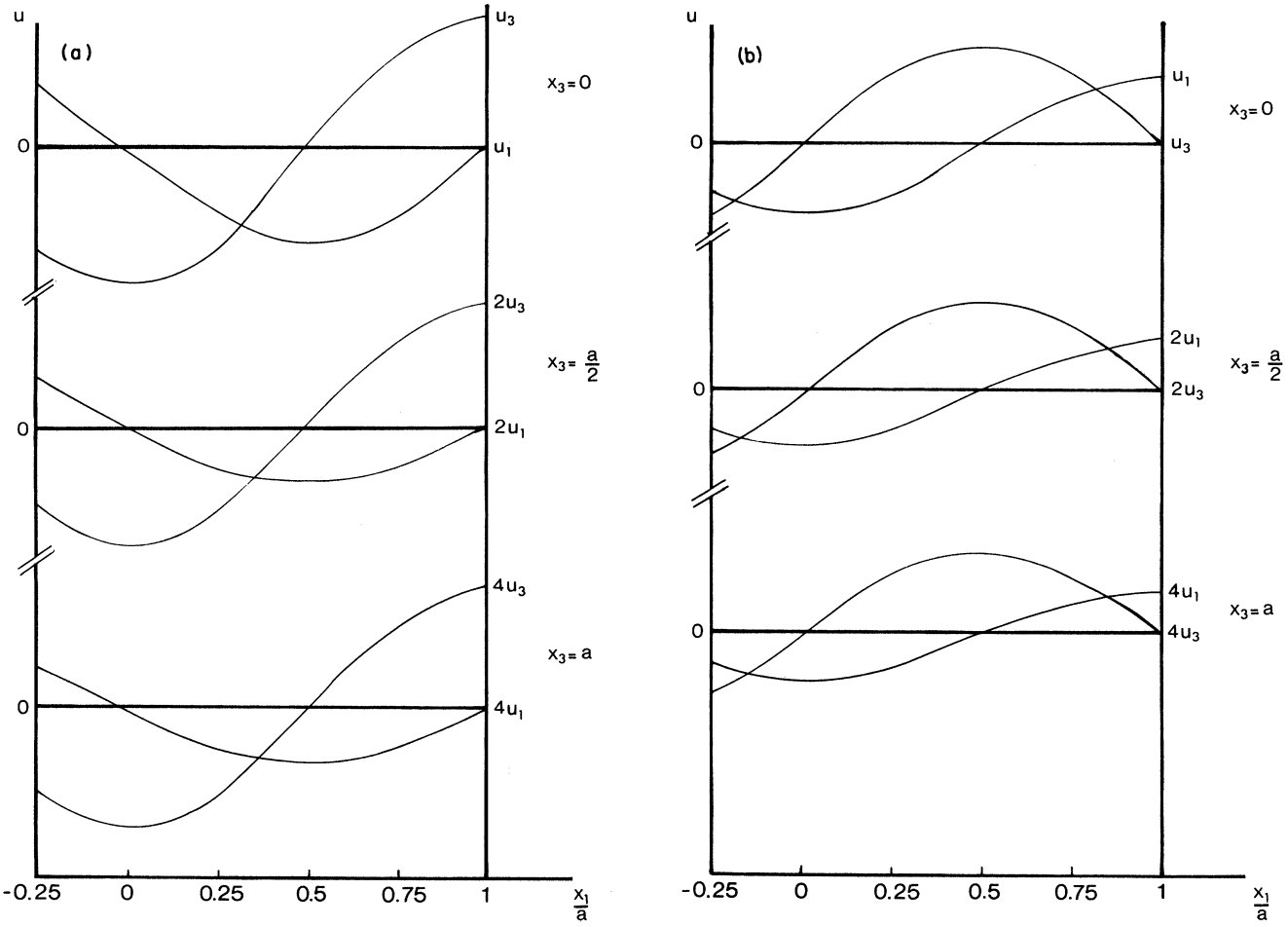

FIG. 6. Displacement fields associated with the (a) lower and (b) upper Rayleigh waves at the point $k = \pi/a$ of Fig. 2(a). The displacements are drawn for different depths from the surface. The displacements are given in arbitrary units.

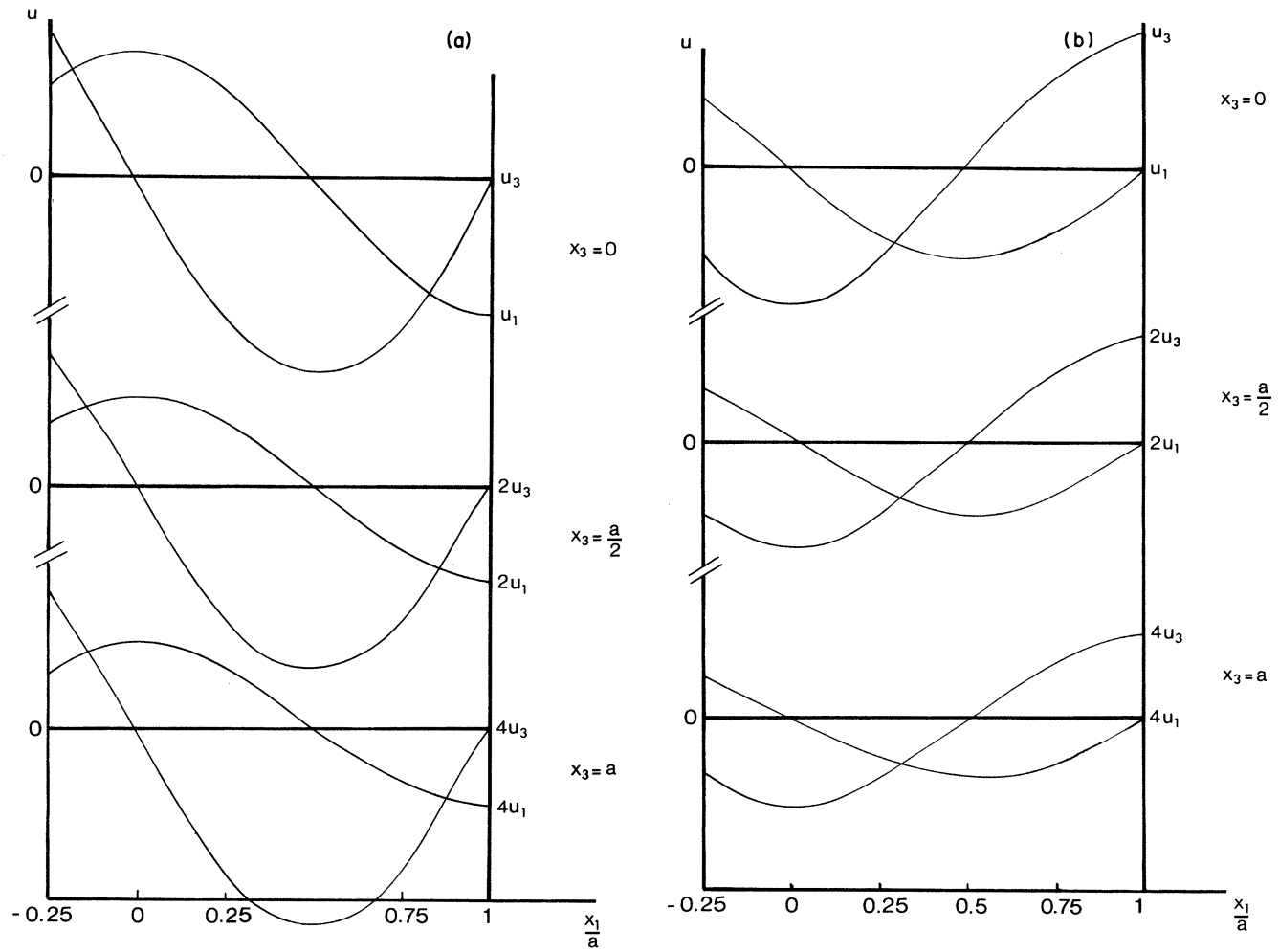

FIG. 7. Displacement fields associated with the (a) lower and (b) upper Rayleigh waves at the point $k = \pi/a$ of Fig. 3(a). The displacements are drawn for different depths from the surface.

higher Rayleigh mode rises in frequency until it disappears completely into the radiative region of the (ω,k) plane. Then one has only the lower branch, as in Figs. 2(b) and 3(b).

As a further illustration of the general structure of the dispersion curves, we present two examples that correspond to more realistic situations. Figure 4 describes a cubic GaAs-$Ga_xAl_{1-x}As$–type superlattice with $\rho'/\rho = 0.9$ and elastic constants identical for the two media ($c_{11} = 11.8$, $c_{12} = 5.35$, and $c_{44} = 5.94$, in units of 10^{10} N/m^2). Figure 5 presents the dispersion curves for a lamellar system of the Al-W type. These are two nearly isotropic crystals having very different parameters (Table II).

B. Displacement field

We present in Figs. 6 and 7 the variations of the displacements u_1 and u_3 [Eqs. (2.16)] along one period of the superlattice for cases (i a) and (ii a) of the preceding subsection for the wave vector k at the Brillouin-zone boundary ($k = \pi/a$). For small wave vectors these variations are slow and we do not present them.

Before discussing these figures, let us emphasize that the displacements [Eqs. (2.16)] are obtained in our calculation for a finite number of their Fourier components. Thus the displacements are continuous at the interfaces between the layers and also have continuous derivatives. However, due to the continuity of the stresses at these interfaces, the derivatives of the displacements should be discontinuous. This property cannot be realized in the numerical analysis, and the behavior of the displacements near the interfaces is approximate.

Figures 6(a) and 6(b) correspond to the lower and upper branches of the Rayleigh-wave dispersion curves of Fig. 2(a) (there is only mass-density variation in the superlattice with $\rho'/\rho = 0.95$). The displacement u_1 associated with the lower (upper) Rayleigh-wave branch has a symmetrical (antisymmetrical) behavior with respect to the midplane of the lighter medium and an antisymmetrical (symmetrical) behavior with respect to the midplane of the heavier medium. The reverse is true for the displacement u_3. In Figs. 6(a) and 6(b) the displacements are presented at the surface and at two different depths inside the crystal, showing the decay of the wave amplitude with increasing distance into the superlattice from the surface.

Similarly, in Figs. 7(a) and 7(b) we have depicted the displacements associated with the lower and upper

branches of the Rayleigh-wave dispersion curves of Fig. 3(a) (only elastic constant variations in the superlattice with $c'_{44}/c_{44}=1.1$) at $k=\pi/a$. The behavior for the lower (upper) Rayleigh-wave branch is similar to that of the upper (lower) wave in Fig. 6.

C. Gap variations versus other parameters

We have seen that for two relatively similar media one obtains, near the zone boundary, two different branches of the Rayleigh-wave dispersion curves that are separated by a gap. Here we will concentrate on the positions of these branches with respect to the bottom of the bulk bands as functions of some parameters in the superlattice at $k=\pi/a$.

Figure 8 presents these two Rayleigh branches as well as the bottom of the bulk bands versus the ratio of the mass density between the two crystals; the elastic constants are in the ratio $c'_{44}/c_{44}=1.1$ The two branches are present in only a limited range of the ratio ρ'/ρ, one of the modes reaching the bulk bands around $\rho'/\rho\cong 0.69$, the other at $\rho'/\rho\cong 1.24$. On the other hand, the two modes become degenerate around $\rho'/\rho\cong 0.96$. Let us remark that if the two crystals differ only by their mass densities, this degeneracy occurs at $\rho'/\rho=1$. The displacements associated with the two modes in Fig. 8 present a behavior similar to that shown in Fig. 7 (Fig. 8) when ρ'/ρ is greater (smaller) than 0.96, which corresponds to the crossing points of the two dispersion curves.

Finally, in Fig. 9 we present the dispersion curves for

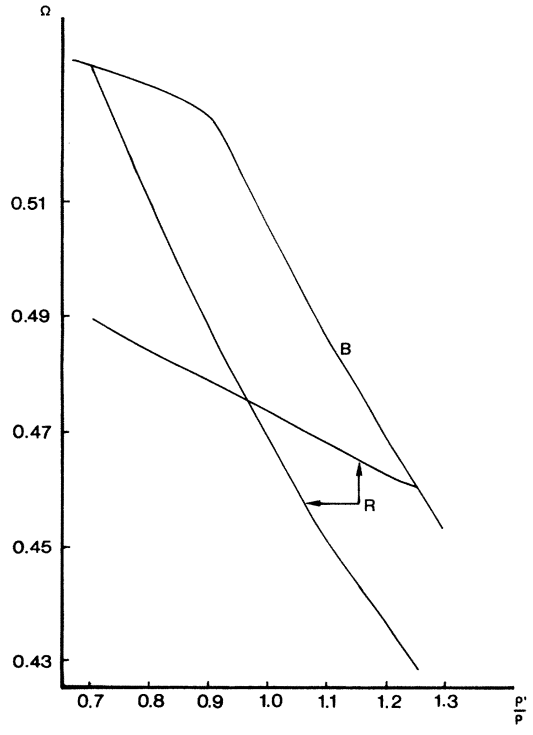

FIG. 8. Bottom of the bulk bands (B) and Rayleigh waves (R) at $k=\pi/a$ versus the ratio of the mass densities of the two media in the superlattice. The layers have the same thickness and their elastic constants are in the ratio $c'_{44}/c_{44}=1.1$. Ω is as defined in Fig. 2.

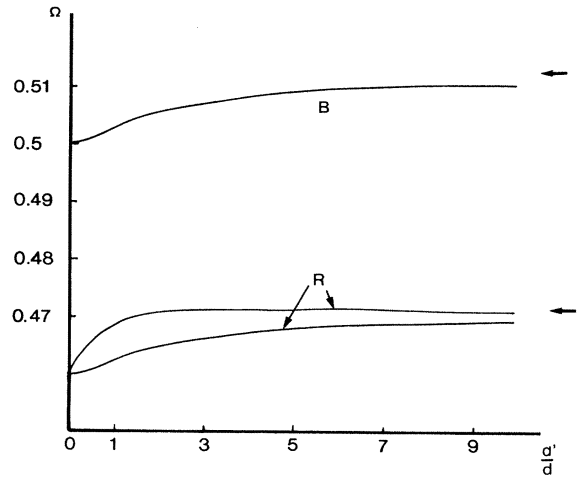

FIG. 9. Bottom of the bulk bands (B) and Rayleigh waves (R) at $k=\pi/a$ versus the ratio of the layer thicknesses. The two media differ only by their mass densities with $\rho'/\rho=0.95$. Ω is as defined in Fig. 2. The arrows indicate the asymptotic limits of the curves for $d'/d\to\infty$.

the Rayleigh wave and the bottom of the bulk bands at $k=\pi/a$ as functions of the ratio between the thicknesses of the two layers. In this example the two media differ only in their mass densities, with $\rho'/\rho=0.95$. At $d'/d=0$, we have a homogeneous medium; departing from this limit, two surface waves appear which then go, in the limit $d'/d\to\infty$, to the Rayleigh wave of the second medium.

IV. CONCLUSIONS

In this paper we have presented a theory of sagittal surface waves on a stratified medium cut perpendicular to the layers. Besides the bending of the modes near the Brillouin-zone boundary, one can observe the folding of the Rayleigh-wave dispersion curve into a second branch if the two media are not very different. The existence of this second branch and its separation from the first branch have been studied as functions of the intrinsic parameters of the media and their thicknesses. The method of the calculation, which is based on a Fourier analysis of the equations of motion in the direction perpendicular to the laminations, shows a better convergence when the two media differ only in their mass densities. This can be understood, at least for small wave vectors where the superlattice becomes equivalent to an effective hexagonal medium.[18] As a matter of fact, the density of this effective medium is the arithmetic mean of the two mass densities, while its elastic constants result from some more sophisticated combinations of the initial elastic constants[18] (for example, the effective c_{44}^{-1} is the arithmetic mean of the two c_{44}^{-1} corresponding to the two layers). Now, the zero Fourier components of the mass density or the elastic constants in the superlattice represent the arithmetic means of these quantities [cf. Eq. (2.6)]. In this long-wavelength limit, the Rayleigh wave of the superlattice is equivalent to that of the effective hexagonal medium cut perpendicular to its isotropic plane.

Finally, we note that we obtained qualitatively similar results to those presented in this paper by modeling the variation of the density and of the elastic constants versus x_1 by sinusoidal functions; however, the convergence of the results is achieved in this last case for smaller values of M. We also note that a method similar to that presented here has been used[19] to study the surface polaritons of a superlattice cut perpendicular to the laminations.

ACKNOWLEDGMENTS

One of the authors (B.D.-R.) would like to thank the Department of Physics of the University of California, Irvine, for its hospitality during the course of this work. This research was supported in part by National Science Foundation Grants Nos. DMR82-14214 and INT 81-15141.

[1]W. M. Ewing, W. S. Jardetzky, and F. Press, *Elastic Waves in Layered Media* (McGraw-Hill, New York, 1957).

[2]L. M. Brekhovskikh, *Waves in Layered Media* (Academic, New York, 1960).

[3]L. Esaki and R. Tsu, IBM J. Res. Dev. 14, 61 (1970).

[4]G. H. Dohler, Phys. Status Solidi 52, 79 (1972).

[5]See, for example, Proceedings of the First International Conference on the Dynamics of Interfaces [J. de Phys. (Paris) Suppl. (to be published)].

[6]R. E. Camley, T. S. Rahman, and D. L. Mills, Phys. Rev. B 27, 261 (1983).

[7]M. Grimsditch, M. R. Khan, A. Kueny, and I. K. Schuller, Phys. Rev. Lett. 51, 498 (1983).

[8]G. F. Giuliani and J. J. Quinn, Phys. Rev. Lett. 51, 919 (1983).

[9]B. A. Auld, G. S. Beaupre, and G. Hermann, Electron. Lett. 13, 525 (1977); B. A. Auld, in *Modern Problems in Elastic Wave Propagation,* edited by J. Miklowitz and Jan D. Achenbach (Wiley, New York, 1978), p. 459.

[10]A. Kueny, M. Grimsditch, K. Miyano, I. Banerjee, C. Falco, and I. Schuller, Phys. Rev. Lett. 48, 166 (1982).

[11]A. Kueny and M. Grimsditch, Phys. Rev. B 26, 4699 (1982).

[12]B. Djafari-Rouhani, L. Dobrzynski, and O. Hardouin Duparc, J. Electron Microsc. Relat. Phenom. 30, 119 (1983); L. Dobrzynski, B. Djafari-Rouhani, and O. Hardouin Duparc, Phys. Rev. B 29, 3138 (1984).

[13]J. Sapriel, B. Djafari-Rouhani, and L. Dobrzynski, Surf. Sci. 126, 197 (1983).

[14]R. E. Camley, B. Djafari-Rouhani, L. Dobrzynski, and A. A. Maradudin, Phys. Rev. B 27, 7318 (1983); J. Vac. Sci. Technol. B 1, 371 (1983).

[15]B. Djafari-Rouhani, L. Dobrzynski, O. Hardouin Duparc, R. E. Camley, and A. A. Maradudin, Phys. Rev. B 28, 1711 (1983).

[16]J. Sapriel, J. C. Michel, J. C. Toledano, R. Vacher, J. Kerverac, and A. Regreny, Phys. Rev. B 28, 2007 (1983).

[17]N. E. Glass, R. Loudon, and A. A. Maradudin, Phys. Rev. B 24, 6843 (1981); N. E. Glass and A. A. Maradudin, J. Appl. Phys. 54, 79 (1983).

[18]S. M. Rytov, Akust. Zh. 2, 71 (1956) [Sov. Phys.—Acoust. 2, 68 (1956)].

[19]N. Glass and A. A. Maradudin, J. Opt. Soc. Am. (to be published).